

BUNCH COMPRESSOR FOR SPring-8 COMPACT SASE SOURCE

Yujong Kim*, T. Shintake, and H. Kitamura, RIKEN, SPring-8, Hyogo 679-5148, Japan
H. Matsumoto, High Energy Research Organization, Ibaraki 305-0801, Japan

Abstract

In the SPring-8 Compact SASE Source (SCSS), the high quality beam with the high peak current and the low emittance should be supplied to saturate the SASE mode within a given undulator length. In this paper, we have described the design concepts of the SCSS bunch compressor.

1 INTRODUCTION

The SCSS project is divided into two phase stages according to the installed components and the radiation wavelength of the SASE source [1], [2]. During the Phase-I stage (2001-2005), the injector, one C-band main linear accelerator, and one bunch compressor (BC) will be installed to generate 40 nm wavelength radiation. During the Phase-II stage (2005-2007), three additional C-band main linear accelerators will be added to generate about 3.6 nm wavelength radiation. Design beam parameters for the two stages are summarized in Table 1, where ϵ_{ns} (ϵ_n) is the slice (projected) transverse normalized rms emittance, $\sigma_{\delta s}$ (σ_{δ}) is the slice (projected) correlated rms relative energy spread. Since electrons being apart further than one cooperation length ($\sim \mu\text{m}$) will not interact with each other, we should focus the slice parameters to predict FEL performance [3], [4]. At the Phase-I stage, we need about 500 A peak current to saturate the SASE-FEL within 13.5 m long undulator. However no present injector technology can directly supply the required high quality beam. Since the peak current is inversely proportional to the bunch length, the required peak current can be obtained by compressing the bunch length. After upgrading the injector system, 4 ps long bunch will be directly supplied to the bunch compressor at the Phase-II stage. And by retuning the operation conditions of the bunch compressor, 2 kA peak current can be obtained by the same bunch compressor. In this paper, we have described the design concepts of the SCSS bunch compressor and how to reduce the beam dilution sources such as coherent synchrotron radiation (CSR) effects and nonlinearities in the longitudinal phase space distribution.

2 COMPRESSOR PRINCIPLE

Bunch compression can be obtained by rotating the bunch in the longitudinal phase space via the two combination actions of the RF precompressor linac and the magnetic chicane. The RF precompressor linac supplies the needed correlated energy spread for the rotation by the energy chirping. When electron with energy spread goes through the chicane, its traveling path length or time is

Table 1: Parameters of SCSS Phase-I and Phase-II stages.

Parameter	Unit	Phase-I	Phase-II
beam energy E	MeV	230	1000
slice normalized emittance ϵ_{ns}	μm	1.6	2.0
projected normalized emittance ϵ_n	μm	2.0	2.5
slice energy spread $\sigma_{\delta s}$	%	0.1	0.02
projected energy spread σ_{δ}	%	2.0	0.4
bunch charge Q	nC	1	1
bunch length before BC $\Delta\tau$ (FW)	ps	8	4
bunch length after BC $\Delta\tau$ (FW)	ps	2	0.5
bunch length after BC Δz (FW)	mm	0.6	0.15
peak current I_{pk}	A	500	2000
saturation length L_{sat}	m	~ 12	~ 20
total undulator length L_{tu}	m	13.5	22.5
cooperation length L_{coop}	μm	~ 1.5	~ 0.2
radiation wavelength λ_x	nm	40	3.6

changed according to its energy, which means the bunch length change [2], [3]. The longitudinal coordinate relation of bunch compression to the second order is given by

$$dz_f = dz_i + R_{56}(dE/E)_i + T_{566}(dE/E)_i^2, \quad (1)$$

$$R_{56} \approx 2\theta_B^2(\Delta L + \frac{2}{3}L_B) = -\frac{2}{3}T_{566}, \quad (2)$$

where dz_f (dz_i) is the longitudinal distance deviation from the bunch center after (before) the chicane, $(dE/E)_i$ is the relative energy deviation before the chicane which is supplied by the precompressor linac, R_{56} is the momentum compaction factor which is supplied by the chicane, T_{566} is the second order the momentum compaction factor due to the second order dispersion of the chicane, θ_B is the bending angle in radian, ΔL is the drift space between the first dipole and the second dipole in the chicane, L_B is the effective length of the dipole in the chicane. Here, we assume that the chicane consists of four rectangular dipoles, and head electrons have positive dz and negative (dE/E) .

3 COMPRESSOR DESIGN CONCEPTS

3.1 Reducing CSR and Nonlinearities

When the bunch length is compressed in the BC, the bunch length may become smaller than the radiation wavelength. In this case, CSR can be generated. Since CSR from tail electrons can overtake head electrons after the overtaking length, head electrons will be accelerated by CSR, and tail electrons will be decelerated due to their own CSR loss. The electrons will be transversely kicked at the nonzero dispersion region due to the CSR-induced correlated energy spread along the bunch. Note the projected emittance can be diluted due to CSR in the bunch compressor while the slice emittance dilution is small enough [3],

* yjkim@spring8.or.jp, http://www-xfel.spring8.or.jp

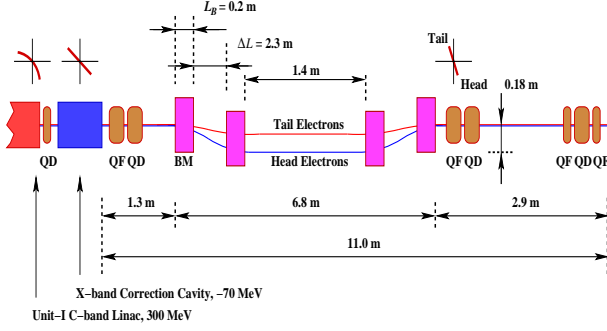


Figure 1: Layout of the SCSS bunch compressor. Here, three long drift sections (before, center, and after BC) are for the beam diagnostics.

[4]. We have reduced the emittance dilution due to CSR in the BC with following methods:

Firstly, after considering the slice emittance dilution in the double-chicane due to the CSR-induced microbunching instability, the slice emittance dilution in the wiggler-combined single chicane due to the spontaneous radiation in wiggler, and the emittance dilution in the S-chicane due to full achromatic difficulty, we have chosen the normal single chicane with four rectangular magnets for our bunch compressor as shown in Fig. 1 [3], [4].

Secondly, we have reduced CSR by the weak strength chicane or small R_{56} [3]. According to Eqs. (1) and (2), this is possible by choosing somewhat large $(dE/E)_i$, the small bending angle, and somewhat large drift space between the first and second dipoles. Optimized parameters of the SCSS BC for the Phase-I and Phase-II stages are summarized in Tables 2 and 3, where the emittance is the rms normalized value, and the energy spread is the rms value. For these optimization, we have used ELEGANT, TraFiC⁴, and PARAO codes [2]. Although the normal operational R_{56} can be reduced further by choosing higher σ_δ , we have chosen $\sigma_\delta \sim 2\%$ to keep the chromaticity-induced projected emittance dilution in linacs within 5%.

Thirdly, we have reduced CSR further by installing the higher harmonic X-band correction cavity before the BC to compensate the nonlinearities in the longitudinal phase space. The X-band correction cavity compensates the second order nonlinearities due to the RF curvature of the C-band linac, the second order path dependence on the particle energy in the chicane, T_{566} , and the short-range wakefields in linacs as shown in Figs.1 and 2 [2], [6]. Here the remain weak nonlinearity after X-band correction cavity is for the T_{566} compensation in the chicane. Since the beam energy is high enough at the SCSS BC, the nonlinearity due to the space charge force can be ignorable. If those nonlinearities are not compensated properly, the local charge concentration or spike is generated during the compression process. This local charge concentration or spike amplifies CSR effects in the bunch compressor [4], [6]. By compensating the nonlinearities with the X-band correction cavity, the limitation of the final obtainable bunch length is also

Table 2: Parameters of the SCSS BC at the Phase-I stage.

Parameter	Unit	Value
beam energy E	MeV	230
initial bunch length Δz_i (FW)	mm	2.4
final bunch length Δz_f (FW)	mm	0.6
initial projected relative energy spread σ_δ	%	2.14
initial uncorrelated relative energy spread $\sigma_{\delta u}$	10^{-5}	~ 5
initial max relative energy deviation $(dE/E)_i$	10^{-2}	3.6
beam phase at the C-band linac ϕ_c	deg	12.5
momentum compaction factor R_{56}	mm	24.8
second order momentum compaction $ T_{566} $	mm	37.2
effective dipole length L_B	m	0.2
drift length between first and second dipoles ΔL	m	2.3
bending angle of each dipole θ_B	rad	0.071
magnetic field of each dipole $ B $	T	0.27
maximum horizontal dispersion η_{max}	m	0.18
maximum horizontal shift Δh	m	0.18
initial slice emittance before BC ϵ_{ns}	μm	1.50
initial projected emittance before BC ϵ_n	μm	1.58
change of slice emittance $\Delta\epsilon_{ns}/\epsilon_{ns}$	%	0.04
change of projected emittance $\Delta\epsilon_n/\epsilon_n$	%	2.3
change of σ_δ due to CSR $\Delta\sigma_{\delta,CSR}$	10^{-4}	2.9
change of slice emittance due to ISR $\Delta\epsilon_{ns,ISR}$	fm	7.6
change of σ_δ due to ISR $\Delta\sigma_{\delta,ISR}$	10^{-8}	6.2

Table 3: Parameters of the SCSS BC at the Phase-II stage.

Parameter	Unit	Value
beam energy E	MeV	218
initial bunch length Δz_i (FW)	mm	1.2
final bunch length Δz_f (FW)	mm	0.15
initial projected relative energy spread σ_δ	%	1.98
initial uncorrelated relative energy spread $\sigma_{\delta u}$	10^{-5}	~ 5
initial max relative energy deviation $(dE/E)_i$	10^{-2}	3.5
beam phase at the C-band linac ϕ_c	deg	24
momentum compaction factor R_{56}	mm	15.0
second order momentum compaction $ T_{566} $	mm	22.5
bending angle of each dipole θ_B	rad	0.056
magnetic field of each dipole $ B $	T	0.20
maximum horizontal dispersion η_{max}	m	0.14
maximum horizontal shift Δh	m	0.14
initial slice emittance before BC ϵ_{ns}	μm	1.50
initial projected emittance before BC ϵ_n	μm	1.54
change of slice emittance $\Delta\epsilon_{ns}/\epsilon_{ns}$	%	0.18
change of projected emittance $\Delta\epsilon_n/\epsilon_n$	%	63.2
change of σ_δ due to CSR $\Delta\sigma_{\delta,CSR}$	10^{-4}	8.7
change of slice emittance due to ISR $\Delta\epsilon_{ns,ISR}$	fm	1.7
change of σ_δ due to ISR $\Delta\sigma_{\delta,ISR}$	10^{-8}	3.8

reduced [2]. However, the X-band correction cavity decelerates the beam about 70 MeV to compensate the nonlinearities [2], [3]. If the S-band linac is used for the pre-compressor linac, the deceleration is reduced to about 18 MeV [2], [6]. The projected emittance dilution due to the transverse short-range wakefield in the X-band correction cavity is within 7% if the misalignment is smaller than 50 μm [6].

Fourthly, the projected emittance dilution can be reduced further by forcing the beam waist close to the fourth dipole, where α -function ($= -0.5\beta'$) is zero [3], [5]. The optimized β -functions are shown in Fig. 3.

Fifthly, although the final bunch length at the Phase-II stage is four times smaller than that of the Phase-I stage, we can control the CSR effects by reducing the chicane strength or R_{56} to 15 mm. This R_{56} can be obtained by keeping σ_δ at the BC about 2% and by supplying 4 ps long

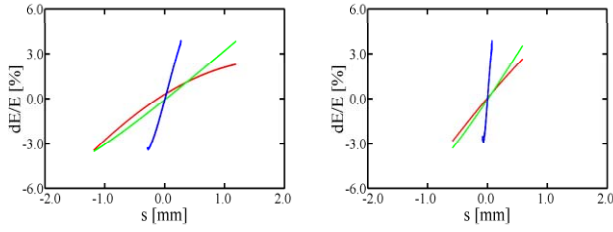


Figure 2: ELEGANT simulation results of the longitudinal phase space distribution at the Phase-I (left) and the Phase-II (right) stages. Red, green, and blue mean the longitudinal phase space distribution after C-band linac, after X-band correction cavity, and after the BC, respectively. The negative s ($= |dz|$) means the bunch head.

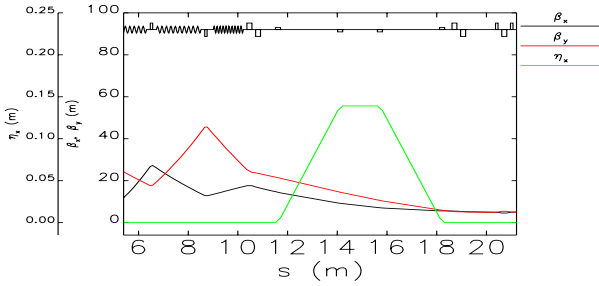


Figure 3: Optimized β -functions of the SCSS BC at the Phase-II stage.

bunch from the injector. We will reduce 2% energy spread to the design value by the longitudinal short-range wakefields in three added C-band main linacs and by operating those linacs close to the RF crest.

Since the initial uncorrelated rms relative energy spread is about 5×10^{-5} , and the spread is also increased in the BC by the random process due to the incoherent synchrotron radiation (ISR) and CSR, the microbunching instability can be ignorable in our weak strength chicane.

3.2 CSR Wake and Emittance Dilution

We have investigated the CSR effects in the bunch compressor for the SCSS Phase-I and Phase-II stages with ELEGANT and TraFiC⁴ codes. The final bunch length and peak current are 0.6 mm and about 500 A at the Phase-I stage, and those of the Phase-II stage are 0.15 mm and about 2 kA, respectively as shown in Figs. 2 and 4. By the help of the X-band correction cavity, the linear densities are good symmetric around the bunch center, and there is no strong spike or the local charge concentration after BC as shown in Fig. 4. The CSR induced correlated energy spread along the bunch is increased as the bunch length is compressed as shown in Fig. 5. Here the head electrons with negative s are accelerated by CSR and the tail electrons are decelerated by their CSR loss. At the Phase-II stage, there is one small special spike around the tail region of the energy change due to CSR or the CSR wake as shown

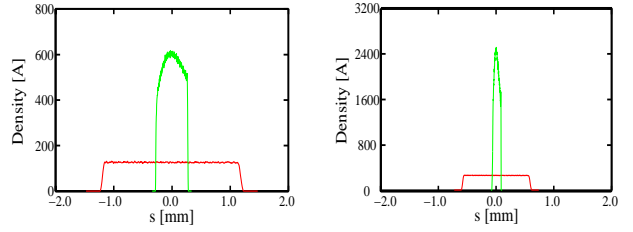


Figure 4: ELEGANT simulation results of the linear density at the Phase-I (left) and the Phase-II (right) stages. Red and green mean the linear density at the end of the first dipole and at the end of the last dipole, respectively.

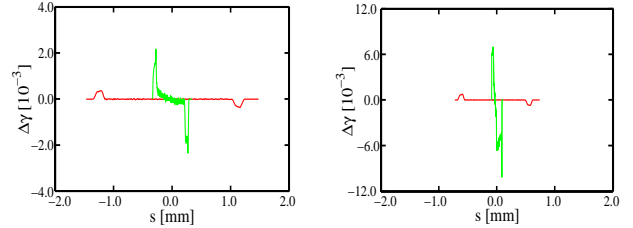


Figure 5: ELEGANT simulation results of the energy change $\Delta\gamma$ due to CSR at the Phase-I (left) and the Phase-II (right) stages. Red and green mean $\Delta\gamma$ at the end of the first dipole, and at the end of the last dipole, respectively.

in Fig. 5(right). This is due to the uncompensated higher order nonlinearities such as the third order term in the longitudinal short-range wakefields and the third order term in the momentum compaction. However our CSR wakes are much smaller than those of other projects. The final slice (projected) normalized rms emittance after BC are about $1.501 \mu\text{m}$ ($1.6 \mu\text{m}$) and $1.503 \mu\text{m}$ ($2.5 \mu\text{m}$) at the Phase-I and Phase-II stages, respectively, which are all within our design values as summarized in Tables 1.

4 SUMMARY

We have reduced the emittance dilution in the bunch compressor by compensating nonlinearities in the longitudinal phase space, by using the weak strength chicane, and by optimizing β -functions in the bunch compressor. The emittance dilutions due to the resistive wall wakefield and the ISR are all small enough to ignore. Sincerely, we thank M. Borland, P. Piot, Z. Huang, P. Emma, A. Kabel, R. Li, and T. Limberg for their discussions and recommendations.

5 REFERENCES

- [1] T. Shintake *et al.*, in these proceedings.
- [2] Yujong Kim, *et al.*, in *Proc. EPAC2002*, Paris, France, 2002.
- [3] LCLS Conceptual Design Report, SLAC-R-593, 2002.
- [4] P. Emma, SLAC Report No. SLAC-PUB-9243, 2002.
- [5] T. Limberg *et al.*, in *Proc. EPAC2002*, Paris, France, 2002.
- [6] P. Emma, SLAC Report No. LCLS-TN-01-1, 2001.